Proceedings of IMECE 2007
2007 ASME International Mechanical Engineering Congress and Exposition
Seattle, Washington, USA, November 11-17, 2007

IMECE2007-41801 Final Version

MULTISCALE CONSTITUTIVE MODEL DEVELOPMENT AND FINITE ELEMENT IMPLEMENTATION FOR MAGNETOSTRICTIVE MATERIALS

William S. Oates
Department of Mechanical Engineering[1]
Florida A&M/Florida State University
Tallahassee, FL 32310-6046
Email: woates@eng.fsu.edu

ABSTRACT

A multiscale constitutive model is developed and applied to magnetostrictive materials to predict multi-axial ferromagnetic switching. The modeling framework is an extension of a one-dimensional homogenized energy model that employs a stochastic distribution of localized magnetic moments. Here, the model is extended to multi-axial ferromagnetic switching in a polycrystalline ferromagnetic material. A mean-field approximation is adopted to quantify ferromagnetic switching from multi-axial magnetic field loading at the single crystal length scale. Polycrystalline ferromagnetic behavior is modeled by homogenizing stochastic distributions of underlying microscopic fields associated with material inhomogeneities at the grain length scale. Approximations of the stochastic distributions are made to improve computational efficiency for finite element implementation. The constitutive model is numerically validated and implemented in the commercial finite element software, COMSOL.

1 Introduction

Magnetostrictive materials are an important class of active materials utilized in many transducer and sensor applications. These materials exhibit changes in the magnetization when external magnetic fields, changes in temperature or stresses are applied. Microscopic magnetic domains rotate or reorient to reduce the Gibbs energy in response to magnetic fields, changes in temperature or stresses. Although significant progress has been made in developing constitutive models for magnetostrictive materials (for examples see [1–6]), efficient multiscale computational models amenable to finite element implementation are limited. The integration of a multiscale active material model into a finite element model is desirable for investigating the effect of local material constituents on macroscale actuator performance when multiaxial loading is present. For example, bimorph actuators undergo in-plane biaxial mechanical bending stress and out-of-plane or in-plane magnetic fields. In addition, compositions such as magnetostrictive Galfenol can be machined or welded [7] which introduces complex loading during the machining process. Moreover, complex geometries, porosity or cracks may be present. Therefore, multi-axial nonlinear and hysteretic constitutive models and finite element integration become more important in quantifying the effect of local field concentrations on the evolution of ferromagnetic switching.

The material mechanisms associated with ferromagnetic switching has been studied extensively, see [1,3,4,8] for a review. Many constitutive models focus on macroscale phenomenological models to formulate a field-coupled constitutive model using macroscale thermodynamic potentials [9]. Other approaches have employed micromagnetics which explicitly incorporate the evolution of local domain structures into a continuum model [1, 4, 10]. In contrast, a stochastic modeling framework has recently been developed and applied to magnetostrictive materials by employing a stochastic distribution of material inhomogeneities [11, 12]. This modeling framework has been successful in quantifying nonlinear and hysteretic ferromagnetic material behavior; however, the constitutive model has been primarily limited to one-dimensional switching behavior. In the one-dimensional model, the macroscopic material behavior is deter-

mined from a distribution of local ferromagnetic moments that switch at different applied magnetic field strengths based on a predefined distribution of coercive fields and local variations in internal fields. As the local magnetic fields approach the local coecive fields, the magnetic moments switch their orientation to reduce the Gibbs energy. These probability distributions are integrated into the constitutive model by employing a finite set of magnetic moments that change their orientation as the applied field changes.

Although this approach to modeling ferromagnetic material behavior has been successful in quantifying nonlinear and hysteretic ferromagnetic switching behavior under uni-axial loading, multi-axial loading is often present. Recently it has been shown that this model framework can be extended to multi-axial electric field loading to predict ferroelectric switching in lead zirconate titanate (PZT) [13]. Approximations of a three dimensional Landau-Devonshire free energy function led to reasonable predictions of multi-axial ferroelectric switching in comparison to data given in the literature [14]. A similar approach is used here where statistical mechanics and continuum thermodynamics are used to develop an effective continuum model used to predict multi-axial ferromagnetic switching. The effective continuum is then implemented in a finite element model.

Section 2 describes the statistical mechanics framework employed to quantify a ferromagnetic single crystal thermodynamic potential. Section 3 extends this energy description to include magneto-static energy and polycrystal behavior. The multiscale model is numerically implemented in Section 4.

2 Statistical Mechanics Relations

Statistical mechanics is often useful in formulating an effective continuum representation of material behavior based on underlying atomistic or quantum properties. This approach is employed here to model single crystal ferromagnetic switching. The Gibbs energy is described by a partition function as

$$G_{ex}(H_i,T) = -kT\ln Z(H_i,T) \tag{1}$$

where H_i is the total magnetic field applied to the single crystal, T is temperature, and k is Boltzmann's constant. Indicial notation has been used where $i = 1,2,3$. The magnetic field is an applied field and an exchange "force" term, $H_i = H_i^a + H_i^{ex}$. The exchange "force" H_i^{ex} is based on an internal field that develops from local spin momentum coupling with quantum effects.

Following [4], the quantum form of the magnetic moments are employed to quantify the microstate partition function. In this case, the magnetic moments have only two states with spin $\pm 1/2$

$$Z_m = \exp\left(\frac{\mu_0(H_i^a+H_i^{ex})m_i}{kT}\right) + \exp\left(-\frac{\mu_0(H_i^a+H_i^{ex})m_i}{kT}\right) \tag{2}$$

where m_i is the magnetic moment and μ_0 is the permeability of free space.

The Gibbs energy is summed over all lattice unit cells N defined by a single crystal representative volume element. Based on (1) and (2), the Gibbs energy is

$$G_{ex}(H_i,T) = -NkT\left\{\ln\left(\cosh\left(\frac{\mu_0(H_i^a+H_i^{ex})m_i}{kT}\right)\right) + \ln(2)\right\}. \tag{3}$$

The magnetization is defined by

$$M_i(H_i,T) = -\frac{1}{\mu_0 V}\left(\frac{\partial G_{ex}}{\partial H_i}\right)_T \tag{4}$$

where V is the representative volume element.

The exchange "force" is assumed to be proportional to the magnetization and given by $H_i^{ex} = \Phi_0 M_i/M_s$ where M_s is the spontaneous magnetization [12]. By substituting the exchange force into (4) and inverting the relation to solve for H_i^a, the Gibbs energy can be rewritten in a form that illustrates the balance between internal energy and entropy which governs the equilibrium ferromagnetic state. Details can be found in [4]. After substitution and manipulating (3) and (4), the Gibbs energy density is

$$\begin{aligned} g_{ex}(H_i,T) = \frac{kNT}{2V}\{&(1+M/M_s)\ln(1+M/M_s)+\cdots \\ &(1-M/M_s)\ln(1-M/M^s)\} - \frac{\Phi_0 N}{4V}\left(\frac{M_i}{M_s}\right)^2 - H_i^a M_i \end{aligned} \tag{5}$$

where $M = \Sigma_i^3\sqrt{M_i^2}$. This form of the Gibbs energy is equivalent to

$$g_{ex}(H_i,T) = u - Ts - H_i^a M_i \tag{6}$$

where u is the internal energy density and s is the entropy density. The internal energy density and entropy density are thus defined by

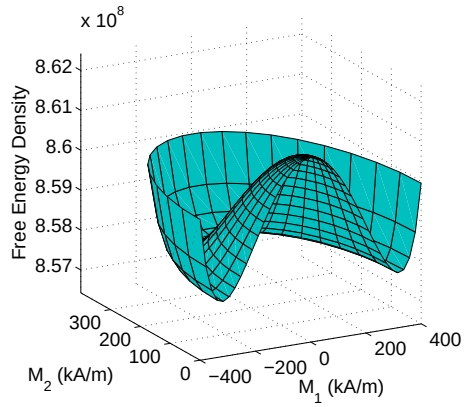

Figure 1. Gibbs free energy density below the Curie temperature ($T < T_c$) based on (5) for zero applied field. Only half of the 2D energy surface is shown to illustrate the low energy magnetization state that occurs about a ring centered at zero magnetization.

$$\begin{aligned} u &= -\frac{H_h M_s}{2}\left(\frac{M_i}{M_s}\right)^2 \\ s &= -\frac{H_h}{2T_c}\{(1+M/M_s)\ln(1+M/M_s)+\cdots \\ &\quad (1-M/M_s)\ln(1-M/M^s)\} \end{aligned} \tag{7}$$

where $H_h = \frac{N\Phi_0}{2VM_s}$ and $T_c = \frac{\Phi_0}{2k}$. The constant internal energy density and entropy density terms have been set to zero since only equilibrium conditions are of interest. Note that a balance between the internal energy and entropy leads to a double-well potential for the one dimensional case. Similar relations hold for two or three dimensions since the exchange energy is only dependent on relative angles between magnetic moments (i.e., no magnetic anisotropy is introduced into the thermodynamic potential). An example of the energy surface is illustrated in Figure 1 for the two dimensional case.

This form of the Gibbs energy density is approximated using piecewise polynomials to improve computational speed in the finite element model. The Helmholtz energy density ($\psi = u - sT$) is given below under isothermal conditions below the Curie temperature

$$\psi_{ex}^{(i)}(M_i) = \begin{cases} \frac{\mu_0}{2\chi_m}(M_i + M^s)^2 & , M_i \le M^I \\ \frac{\mu_0}{2\chi_m}(M^I - M^s)\left(\frac{M_i^2}{M^I} - M^s\right) & , |M_i| < M^I \\ \frac{\mu_0}{2\chi_m}(M_i - M^s)^2 & , M_i \ge M^I \end{cases} \tag{8}$$

$$\psi_{ex}(M_i) = \sum_{i=1}^{3} \psi_{ex}^{(i)} \tag{9}$$

where χ_m is the magnetic susceptibility in the region near the energy well. M^I is the positive inflection value. This form of the Helmholtz energy density results in double-well potentials in each direction $i = 1$ to 3 at temperatures below the Curie temperature. The total Helmholtz energy is obtained by summing the components in each direction as given by (9). This approximates the Gibbs energy density, $g_{ex} \simeq \psi_{ex} - H_i^a M_i$. The approximate form of the Gibbs energy is used in the following section to quantify ferromagnetic switching in a polycrystalline ferromagnetic material.

3 Effective Continuum Model

In this section, the model is extended to include magneto-static self energy and polycrystalline behavior. First magneto-static energy is introduced at the single crystal length scale. The additional energy term gives rise to two sets of coupled equations that are incorporated into the finite element model. Second, a homogenization technique is introduced to quantify the effect of polycrystal inhomogeneities on ferromagnetic switching.

Magneto-static energy is added to the Helmholtz energy density

$$\begin{aligned} \psi &= \psi(B_i, M_i) \\ &= \psi_{ex}(M_i) + \psi_{mag}(B_i, M_i) \end{aligned} \tag{10}$$

where $\psi_{mag}(B_i, M_i)$ is magnetic self energy and B_i is magnetic induction. Only isothermal conditions below the Curie temperature are considered; therefore, temperature does not contribute to the equilibrium magnetization state and is neglected in subsequent relations.

The magnetic self energy is defined by

$$\psi_{mag}(B_i, M_i) = \frac{\mu_0}{2}\left(\frac{B_i}{\mu_0} - M_i\right)^2. \tag{11}$$

The Gibbs free energy density is used to write the thermodynamic potential as a function of magnetization and field. This reduces the number of degrees of freedom required for finite element implementation; see [15] for a similar approach for ferroelectric materials.

$$g(M_i, H_i) = \psi(B_i, M_i) - H_i B_i \tag{12}$$

and the work conjugate variables are

$$H_i^I = \frac{\partial g}{\partial M_i} \quad \text{and} \quad B_i = -\frac{\partial g}{\partial H_i} \tag{13}$$

where the field H_i^I is due *only* to the magnetized body and the magnetic induction is B_i. The magnetic field due to the magnetic body is distinguished from the total field and the applied field H_i by the relation, $\overline{H}_i = H_i + H_i^I$. The field H_i^I will be denoted as an "interaction" field and used in formulating the homogenization framework in subsequent equations.

The minimization of (12) leads to two sets of equations governing the ferromagnetic constitutive behavior. Since only quasi-static fields are considered, the current density is negligible and the magnetic field can be written in terms of a magnetic potential, $\overline{H}_i = -\phi^m_{,i}$. These relations are substituted into (12) and the variation of the Gibbs free energy density at equilibrium is

$$\delta g = \frac{\partial g}{\partial M_i}\delta M_i + \left(\frac{\partial g}{\partial \phi^m_{,i}}\right)_{,i} \delta\phi^{mag} \geq 0 \tag{14}$$

where calculus of variations has been used in the substitution.

Since magnetization and the magnetic potential are independent variables, two sets of governing equations must be satisfied at equilibrium

$$\begin{aligned} \frac{\partial g}{\partial M_i} &= 0 \\ \left(\frac{\partial g}{\partial \phi^m_{,i}}\right)_{,i} &= B_{i,i} = 0 \end{aligned} \tag{15}$$

where the first equation, $(15)_1$, governs the evolution of the magnetization at the single crystal length scale and $(15)_2$ is Maxwell's equation for divergent free magnetic induction.

3.1 Polycrystal Model

Whereas the previous relations describe single crystal ferromagnetic material behavior, significant variations in the constitutive behavior can occur in a polycrystal material. For example, variations in crystal anisotropy between grains, intergranular residual stress, or grain size effects may contribute to differences in ferromagnetic switching. Explicit representations of this material behavior at the macroscopic length scale is challenging, therefore, a stochastic modeling framework is implemented to quantify these effects.

A stochastic homogenization framework is introduced to quantify an effective continuum. The magnetic induction is homogenized based on an underlying probability distribution of internal fields and coercive fields

$$\overline{B}_i(M_j, H_j) = \int B_i(M_j, \overline{H}_j)\nu(H_j^I; H_j^c) dH_j^I dH_j^c \tag{16}$$

where $\nu(H_j^I; H_j^c)$ is the probability distribution of a set of interaction fields H_j^I and coercive fields H_j^c which are introduced to describe polycrystal material inhomogeneities. This relation can be simplified by substituting, $B_i = \mu_0(\overline{H}_i + M_i)$, and solving for magnetization as a function of applied field. The interaction field probability distribution is assumed to be symmetric about zero field and therefore does not contribute to the integral equation. The homogenized magnetization and induction is then

$$\begin{aligned} \overline{M}_i(H_j) &= \int M_i(\overline{H}_j)\nu(H_j^I; H_j^c) dH_j^I dH_j^c \\ \overline{B}_i &= \mu_0(H_i + \overline{M}_i) \end{aligned} \tag{17}$$

A similar form for the one dimensional case is described in detail in [11, 12].

The distribution of interaction fields and coercive fields affect the evolution of single crystal magnetic variant reorientation when external fields are applied. This requires integrating over local fields and coercive fields in three dimensions which presents numerical challenges when implementing (17) in a finite element model. Approximations of the probability distributions are introduced to improve computational speed.

Whereas material inhomogeneities are often described by a distribution of both internal magnetic fields and coercive fields, this does not necessarily give a unique probability distribution. For example, the coercive field distributions correspond to the fields required to switch single crystal magnetic variants which may vary for each grain in the polycrystal. As a magnetic field is applied, a magnetic variant will switch when the applied field plus the interaction field H_i^I equals the single crystal coercive field. These distributions are not necessarily unique since a different interaction field and coercive field will give ferromagnetic switching at the same applied field. The model presented here assumes a constant coercive field. Material inhomogeneities are proposed to be a function of only the interaction field probability

distribution. This distribution is assumed to be a normal distribution with zero mean. The coercive field is assumed to be a constant vector (i.e., Dirac delta distribution).

The probability distributions utilized in the model are

$$\nu_1(H_i^I;H_i^c) = cH_i^c\delta(H_i - H_i^c)e^{-(H_i^I)^2/2b^2}. \tag{18}$$

where $\delta(H_i - H_i^c)$ is the Dirac delta function and c is a scaling constant to ensure the integration of the probability distribution is equal to one. The introduction of the Dirac delta distribution simplifies the dependence on H_i^c which can be integrated out of (17). For the two dimensional case, the homogenized magnetization reduces to

$$\begin{aligned}\overline{M}_1(H_1,H_2) &= \int_{-\infty}^{\infty}\int_{-\infty}^{\infty} M_1(\overline{H}_1,\overline{H}_2)\nu(H_1^I,H_2^I)dH_1^I dH_2^I \\ \overline{M}_2(H_1,H_2) &= \int_{-\infty}^{\infty}\int_{-\infty}^{\infty} M_2(\overline{H}_1,\overline{H}_2)\nu(H_1^I,H_2^I)dH_1^I dH_2^I\end{aligned} \tag{19}$$

It should be noted that the coercive field still affects the switching behavior on M_i. This is discussed in the following section.

In summary, the homogenized magnetization is determined using (19) and is integrated into the finite element model to determine ferromagnetic switching behavior when multi-axial fields are present. This approximates the ferromagnetic switching process by applying a homogeneous magnetization at every finite element node.

4 Numerical Implementation

4.1 Constitutive Model

The constitutive equations described in the previous section are numerically implemented to quantify ferromagnetic switching during multiaxial field loading. The approximate form of the Helmholtz energy density given by (9) is utilized to obtain the local magnetization $M_i(\overline{H}_j)$ that is implemented in (19). Numerical examples of the constitutive model are given and then implemented in the finite element model.

Whereas the magnetization given by (4) can be used to quantify magnetization, the simplified energy function given by (8) is used to define single crystal magnetization. The minimization of (8) gives

$$M_i = \chi_m\overline{H}_i + \delta_i(\overline{H}_j;\overline{H}_j^c)M_s \tag{20}$$

which is defined as the local magnetic variant summed over all magnetic moments in the single crystal representative volume element. The function δ_i is restricted to values between -1 and 1 and the additional relation, $\sqrt{\delta_1^2+\delta_2^2+\delta_3^2} = 1$. Here, we assume the switching function $\delta_i(\overline{H}_j;H_j^c)$ is decoupled from mechanical loading and therefore limited to operating regimes where "ferroelastic" or stress induced ferromagnetic switching is negligible. Moreover, energy barriers to switching are imposed on $\delta_i(\overline{H}_j;H_j^c)$ which is not explicitly described by the energy function illustrated in Figure 1 where magnetic moments are free to rotate in certain directions. The model used here assumes that constraints from surrounding grains limit the direction magnetic moments can switch and therefore introduce energy barriers for switching.

The local magnetization given by (20) is implemented numerically to illustrate how the constitutive model is implemented in a finite element framework to quantify multi-axial switching behavior. We assume that single crystal magnetic variants can reorient in the direction of the applied field. Using this approximation, the local magnetic variants δ_i rotate to align with the applied field when the local field is equal to or greater than the coercive field according to

$$\delta_i^{sw} = \frac{\overline{H}_i}{\sqrt{\overline{H}_j\overline{H}_j}}. \tag{21}$$

The local variants are the unit normals in the direction of field. The variants $\delta_i(\overline{H}_j,H_j^c) = \delta_i^{sw}$ when $\sqrt{(\overline{H}_1)^2+(\overline{H}_2)^2+(\overline{H}_3)^2} \geq H_i^c$ and otherwise, $\delta_i(\overline{H}_j,H_j^c)$ remains constant under changes in the external field. This defines an average yield surface as a sphere; however, the local fields and switching behavior are assumed to vary based on the probability distribution ν previously given by (18).

The relations given by (18)-(21) provide the necessary equations to determine the homogenized magnetization for a given magnetic field. As detailed in [12], the implementation of (19) requires approximation of the integrals. This can be done by implementing Gaussian quadrature routines over infinite or semi-infinite domains. The model can be discretized in the following form

$$\overline{M}_i(H_1,H_2) = \sum_{K=1}^{N_K}\sum_{L=1}^{N_L} M_i\nu(H_{1(K)}^I,H_{2(L)}^I)r_K w_L \tag{22}$$

for $i = 1,2$ and r_K and w_L are the respective quadrature weights for $K = 1$ to N_K and $L = 1$ to N_L. An example of the hysteresis under multi-axial loading is given in Figure 2. In this case, the field was applied at an angle 30^o from the x_2 direction given in the figure. The macroscopic magnetization in the x_1 and x_2 direction is shown.

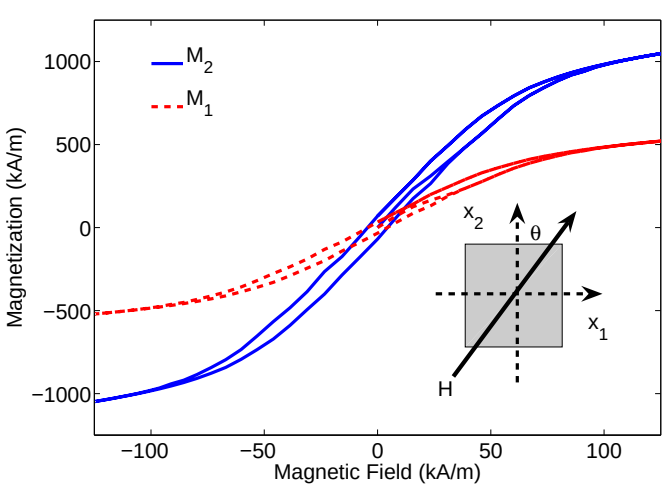

Figure 2. Ferromagnetic constitutive model result using the multi-axial homogenized energy model. The field is applied at an angle of $\theta = 30^o$ relative to the x_2 direction. The magnetization components are plotted versus the magnitude of applied field, $|H|$.

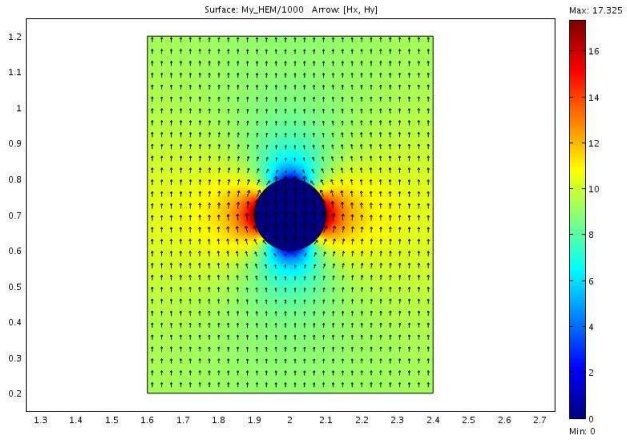

Figure 3. Nonlinear finite element model prediction of macroscopic magnetization using the multiscale energy model. The field component M_2 is plotted and arrows represent the field lines. A zero magnetic potential is applied across the bottom surface and $\phi^m = -1$ A on the top surface, resulting in an external field $H_2^\infty = 1$ kA/m. The sides of the model are magnetically insulating.

4.2 Finite Element Implementation

The multiscale energy model is coupled with the finite element package COMSOL to quantify macroscale ferromagnetic switching. The circular hole problem is used to illustrate how the model predicts ferromagnetic switching when multi-axial fields are present. Finite element nodal solutions for the magnetic potential are computed based on homogenized magnetization $\overline{M}_i(H_j)$ and solved using the GMRES geometric multigrid solver in COMSOL. The finite element model is based on Maxwell's equation previously given by $(15)_2$; however, here the homogenized form of the magnetic induction is used in the finite element model. By substituting $\overline{B}_i = \mu_0(-\phi^m_{,i} + \overline{M}_i(H_j))$ into $\overline{B}_{i,i} = 0$, the weak form of the problem for the two dimensional case is

$$\begin{aligned}
&\int_\Omega \frac{\partial w}{\partial x_1}\left(-\mu_0\left(-\phi^m_{,1} + \overline{M}_1(H_1,H_2)\right)\right) + \cdots \\
&\frac{\partial w}{\partial x_2}\left(-\mu_0\left(-\phi^m_{,2} + \overline{M}_2(H_1,H_2)\right)\right) dx_1 dx_2 + \cdots \\
&\int_\Gamma w\mu_0\left(\left(-\phi^m_{,1} + \overline{M}_1(H_1,H_2)\right)n_1 + \left(-\phi^m_{,2} + \overline{M}_2(H_2)\right)n_2\right) ds = 0
\end{aligned} \tag{23}$$

where w is the weight function, Ω is the domain of the ferromagnetic 2D body and Γ is on the boundary denoted by s. The unit normals are n_1 and n_2 in the x_1 and x_2 directions, respectively.

Results of the nonlinear finite element problem are given in Figures 3-6. The hole is defined to be a void with permeability of free space properties surrounded by the ferromagnetic material. A zero magnetic potential is applied to the bottom surface. A uniform field in the x_2 direction is applied starting from the demagnetized state. The external field is ramped up to $H_2^\infty = 1$ kA/m. This induces a field concentration near the hole as illustrated in Figure 3. The average magnetization away from the hole was verified to be comparable to the values illustrated in Figure 2 when $\theta = 0$.

Numerical validation has been conducted to ensure self-consistency between the finite element model and multiscale energy model. For uniform field loading in the absence of a circular hole, the constitutive model prediction and finite element solutions are within the finite element convergence criterion and has been validated for multiple load and unload steps when ferromagnetic nonlinearities and hysteresis depicted in Figure 2 are present.

To further validate the model, the external field applied in Figures 3 and 4 is reduced to zero and remanent magnetization near the hole is computed. It is interesting to note that demagnetizing fields illustrated in Figure 6 induce reverse ferromagnetic switching on the top and bottom of the hole as shown in Figure 5.

5 Concluding Remarks

A multiscale energy modeling framework has been introduced and applied to predict ferromagnetic switching in magnetostrictive materials. Statistical mechanics was used to quan-

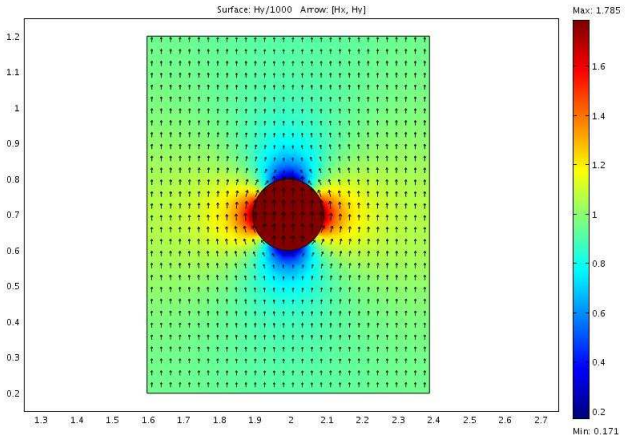

Figure 4. Nonlinear finite element model illustrating the magnetic field in the x_2 direction which corresponds to the magnetization illustrated in Figure 3. Again the external field $H_2^{\infty} = 1$ kA/m was applied.

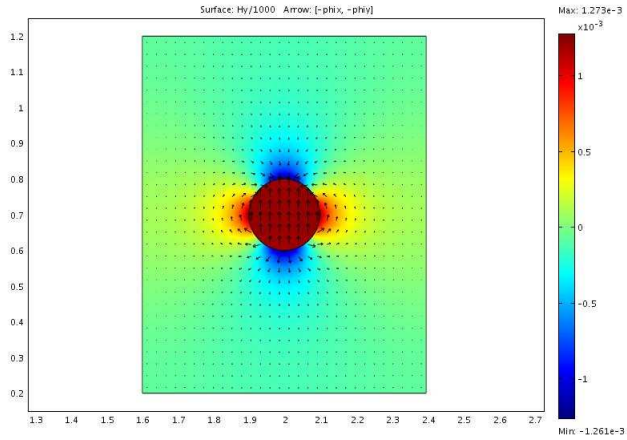

Figure 6. Finite element results illustrating magnetic field in the x_2 direction when the remanent magnetization illustrated in Figure 3 is present. Again, the original external field $H_2^{\infty} = 1$ kA/m applied was reduced to zero.

tify a free energy function at the single crystal length scale. Approximations of the energy function led to a simplified form of the constitutive law that was implemented numerically. Whereas certain numerical algorithms such as quasi-Newton can be implemented to obtain the minimum energy, it has been shown that employing the piecewise polynomial representation of the free energy given by (8) can lead to two to three orders of magnitude increase in computational speed [13]. Approximations to the higher order energy are desired to implement the model into a finite element framework; therefore, the piecewise polynomials were introduced to approximate the energy function. Using this approach, reasonable constitutive behavior was predicted with sufficient computational speed.

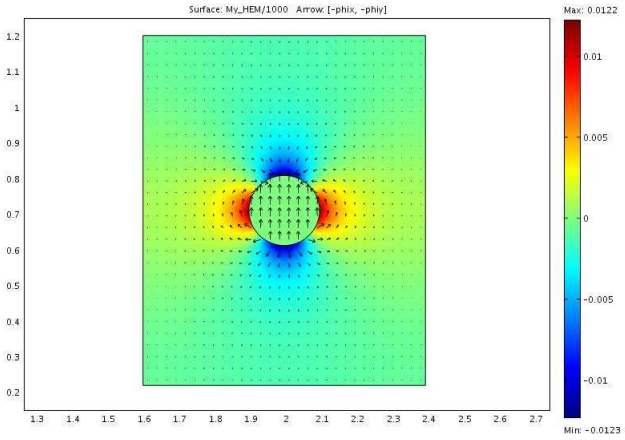

Figure 5. Finite element model prediction of magnetization when the field is reduced to zero. The field component M_2 is again plotted and arrows represent the field lines. Remanent magnetization is shown in regions near the circular hole.

The homogenized form of the magnetization was coupled to the finite element model to quantify ferromagnetic switching behavior for a circular hole problem with free space properties in the hole. The finite element model assumes that the material is statistically homogeneous where the same probability distribution can be applied to each finite element. This is a reasonable approximation for quantifying macroscopic material behavior; however, in situations such as a field concentration near a crack tip, further work is required to assess the approximation used in homogenizing each finite element as the size of the finite element approaches the microscopic or sub-microscopic length scale. This is expected to have significant effects on the form of the probability distribution. An approach similar to the quasi-continuum method described in [16] may be needed.

The Gibbs free energy given by (12) only includes exchange energy and magneto-static energy. Anisotropy energy associated with the crystal structure was neglected. Current work is focused on integrating anisotropy energy into the model to incorporate ferromagnetic switching behavior that tends to align with the easy axis defined along certain crystallographical orientations.

6 Ackowledgements

The author gratefully acknowledges support through the subcontract with Etrema Products, Inc. provided by the Office of Naval Research. The author also wishes to acknowledge several insightful discussions with Ralph Smith (North Carolina State University) and Anter El-Azab (FAMU-FSU).

REFERENCES

[1] Brown, W., 1966. *Magnetoelastic Interactions*. Springer-Verlag, Berlin.

[2] Jiles, D., 1991. *Introduction to Magnetism and Magnetic Materials*. Chapman and Hall, New York.

[3] Aharoni, A., 1996. *Introduction to the Theory of Ferromagnetism*. Oxford Science Publications, New York.

[4] Bertotti, G., 1998. *Hysteresis in Magnetism: for Physicists, Materials Scientists, and Engineers*. Academic Press, San Diego, CA.

[5] Armstrong, W., 2002. "A directional magnetization potential based model of magnetoelastic hysteresis". *J. Appl. Phys.,* **91**(4), pp. 2202–2210.

[6] Dapino, M., Calkins, F., and Flatau, A., 1999. "Magnetostrictive devices". In *Wiley Encyclopedia of Electrical and Electronics Engineering*, J. Webster, ed., Vol. 12. John Wiley and Sons, New York, pp. 278–305.

[7] Ueno, T., Summers, E., and Higuchi, T., 2006. "Machining of iron-gallium for microactuator". *Proc. SPIE Active Materials: Behavior and Mechanics,* **6170**, pp. 61700O–1–61700O–8.

[8] Kittel, C., 1949. "Physical theory of ferromagnetic domains". *Rev. Mod. Phys.,* **21**(4), pp. 541–583.

[9] Wan, Y., Fang, D., and Hwang, K.-C., 2003. "Non-linear constitutive relations for magnetostrictive materials". *Int. J. Non-linear Mech.,* **38**, pp. 1053–1065.

[10] Zhang, J., and Chen, L., 2005. "Phase-field microelasticity theory and micromagnetic simulations of domain structures in giant magnetostrictive materials". *Acta Mater.,* **53**, pp. 2845–2855.

[11] Smith, R., Seelecke, S., Dapino, M., and Ounaies, Z., 2006. "A unified framework for modeling hysteresis in ferroic materials". *J. Mech. Phys. Solids,* **54**(1), pp. 46–85.

[12] Smith, R., 2005. *Smart Material Systems: Model Development*. SIAM, Philadelphia, PA.

[13] Oates, W., and Smith, R. "Multi-axial homogenized energy model for ferroelectric materials". *Proc. ASME IMECE 2006, to appear*.

[14] J.E.Huber, and N.A.Fleck, 2001. "Multi-axial electrical switching of a ferroelectric: theory versus experiment". *J. Mech. Phys. Solids,* **49**, pp. 785–811.

[15] Su, Y., and C.Landis, 2007. "Continuum thermodynamics of ferroelectric domain evolution: Theory, finite element implementation and application to domain wall pinning". *J. Mech. Phys. Solids,* **55**, pp. 280–305.

[16] Miller, R., and Tadmor, E., 2002. "The quasicontinuum method: Overview, applications, and current directions". *J. Comput-Aided Mater.,* **9**, pp. 203–239.